

Evidence for Bose liquid from anomalous shot noise in nanojunctions of bad metal β -Ta

Yiou Zhang,^{1,*} Chendi Xie,^{2,†} John Bacsá,² Yao Wang,² and Sergei Urazhdin¹

¹*Department of Physics, Emory University, Atlanta, Georgia 30322, USA*

²*Department of Chemistry, Emory University, Atlanta, Georgia 30322, USA*

(Dated: June 12, 2025)

We report anomalous shot noise in nanojunctions of β -tantalum, a “bad” metal whose electronic properties are inconsistent with the Fermi liquid theory. Fano factors cluster around even multiples of the values expected for Fermi liquids, suggesting that β -Ta may host a correlated charge liquid of Cooper pair-like electron groups. Further evidence for correlations is provided by the effects of magnetic impurities, as well as reduced density of states near the Fermi level indicated by point contact spectroscopy and first principles calculations. Our results open new avenues for studies and applications of electron correlations.

Introduction. Exotic electronic states not described by the single-particle Fermi liquid (FL) picture can emerge close to the quantum critical points (QCPs) such as metal-insulator transition (MIT) [1]. The resistivity of materials termed “bad” metals is close to the Ioffe-Regel localization limit and typically shows a small increase with decreasing temperature T , indicating proximity to MIT. Bad metallicity is observed in a wide range of materials, including unconventional superconductors [2–4] and other strongly correlated metals [5–9].

The non-divergent negative temperature coefficient of resistivity (TCR) is inconsistent with both single-electron localization and diffusive transport. Thus, “bad” metals are sometimes termed “weak” or “failed” insulators [10, 11]. These behaviors were hypothesized to originate from electron correlations, whose nature remains unsettled [10, 12, 13]. Anomalous properties of some superconducting (SC) bad metal films close to the critical temperature T_C [14–17] were attributed to a correlated state termed the Bose liquid [10, 12, 18–22], which may host incoherent Cooper pairs [11] or a condensate that lacks long-range phase coherence [23].

Since many-particle entanglement is expected close to QCPs such as MIT [24], can Bose liquid exist in “bad” metals that do not superconduct, or at $T \gg T_C$? We address this question by studying shot noise (SN) in nanojunctions of β -Ta, a “bad” metal with $T_C < 0.5$ K widely utilized in spin-orbitronics due to its large spin Hall effect (SHE) [25]. SN is white noise caused by the discrete nature of charge carriers. For a tunnel junction (TJ), its current spectral density is $S_I = 2FeI$, where I is current, $F = q/e$ is the Fano factor, q is the charge of elementary excitations and e is the electron charge [26]. The value of F provides information about the nature of charge carriers, as exemplified by doubling of F due to Cooper pairing [27, 28], or rational F in fractional quantum Hall systems [29, 30]. Enhanced F observed in the normal state of disordered [31] and high-temperature superconductors [32] supported the Bose liquid picture.

SN in metallic junctions (MJs) provides an alterna-

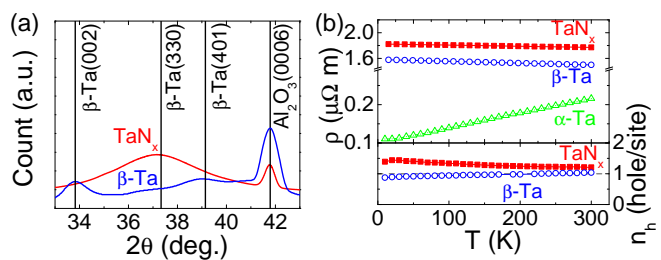


Figure 1. (a) XRD $\theta-2\theta$ scan on β -Ta and TaN_x using Co $K\alpha$ line. (b) Resistivity and Hall data for β -Ta (solid symbols) and TaN_x (open symbols). Resistivity of α -Ta (triangles) grown on a Ti(1) buffer without N_2 is shown for comparison. The thickness of all films was 15 nm.

tive method for the characterization of electron correlations, although it is complicated by the effects of electron-phonon interaction [33]. Nevertheless, SN suppression in “strange” and “bad” metal nanowires [34, 35] was interpreted as a signature of a correlated electron liquid that lacks single-electron excitations [36].

Here, we report anomalously large SN in both TJs and MJs based on β -Ta, providing evidence for the correlated Bose liquid state. This interpretation is supported by complementary measurements and first principles calculations. Our results open new avenues for the studies and applications of correlated materials.

Methods. To obtain a well-defined β -phase, Ta was sputtered in the presence of a small partial pressure of nitrogen $P_N = 4 \times 10^{-6}$ Torr, resulting in a highly disordered microcrystalline structure as reflected by the broad x-ray diffraction (XRD) peak identified as β -Ta (330) (Fig. 1(a)). No α -Ta or crystalline TaN phases were detected, but energy dispersive spectroscopy showed that a small amount of nitrogen became incorporated in the film, forming TaN_x with $x = 9 \pm 2\%$ (see Supplemental Materials, SM). Hall measurements give one hole per atom in β -Ta, and a slightly higher hole concentration in TaN_x consistent with nitrogen doping. The mean free path is only slightly reduced by disorder (see SM). The

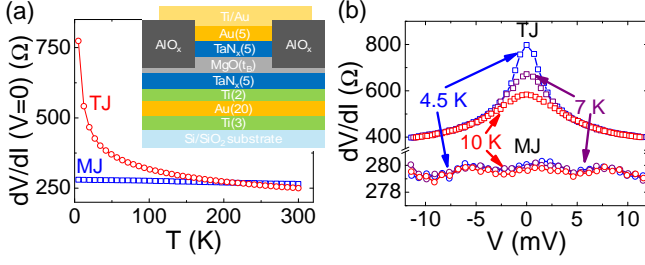


Figure 2. R vs T (a) and V (b) for a TJ and MJ, as labeled. Inset in (a) is the cross-section schematic of the junctions.

resistivity slightly increases but remains non-divergent, as expected for “bad” metals (Fig. 1(b)). The small effect of disorder on electronic properties confirms that bad metallicity in β -Ta cannot be explained by disorder-driven single-electron localization.

The studied junctions were based on multilayers formed by two TaN_x electrodes separated by an MgO tunnel barrier and sandwiched between highly conducting electrodes, inset in Fig. 2(b). Barrier thickness, $t_B = 2.9$ nm for TJs and 3.5 nm for MJs, was chosen so that the resistances R of TJs and MJs were comparable, maximizing the sensitivity of our noise measurement setup optimized for $R = 0.2 - 2$ k Ω . The films were vacuum-annealed at 300 °C for 2 hours and patterned into micron-scale junctions by e-beam lithography. The quality of TJs was confirmed by the decrease of R with increasing T or bias voltage V (Fig. 1(c),(d)), consistent with the Fowler-Nordheim theory [37].

MJs were naturally formed in some samples due to pinholes in the tunnel barrier, but they were not sufficiently stable for SN measurements. The studied MJs were formed by applying voltage pulses until junction resistance dropped to $R \approx 300$ Ω . The latter was almost independent of T and V (Fig. 1(c),(d)), consistent with metallic conduction through nanoscale pinholes. The length of MJ is no larger than $t_B = 3.5$ nm, avoiding electron-phonon scattering effects that can compromise SN measurements in nanowires [35].

Voltage noise S_V was measured by cross-correlation technique, as reported elsewhere [36]. The calibration and measurement approaches were verified using Al/AlO_x/Al TJs, yielding Fano factor $F = 1$ as expected for single-electron tunneling between Al electrodes (see SM). The noise spectra were analyzed to elucidate the contribution from the flicker noise (FN), which identified by $1/f$ spectrum, quadratic increase with bias, and increase with T [38] (see SM for details).

Results. Figures 3(a)-(d) show $S_I(V) = S_V/(dV/dI)^2$ for two TJs and two MJs. 9 additional TJs and 7 MJs show similar behaviors in the range of T and V limited by the onset of FN (see SM for details). For all the junctions, the noise increases

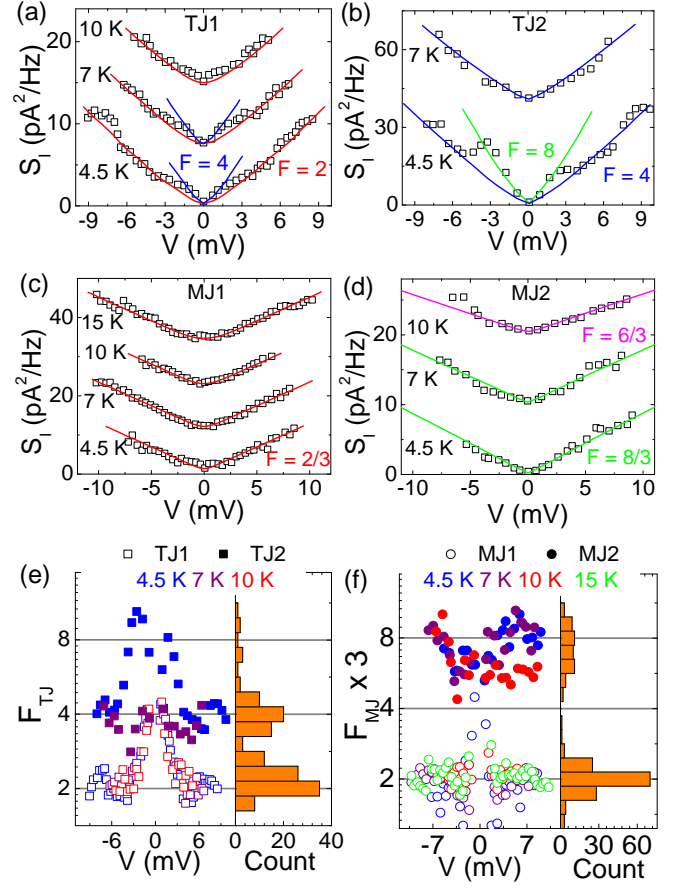


Figure 3. (a)-(d) Shot noise vs bias for two TJs (a),(b) and MJs (c),(d), at the labeled T . The noise data for different temperatures are offset for clarity. The curves are fittings with Eq. (1) for TJs and Eq. (2) for MJs. (e),(f) F vs bias for TJs (e) and MJs (f), and histograms of the corresponding distributions.

approximately linearly with bias above a few mV, consistent with the expectations for SN. The data were fitted with

$$S_I(V) = \frac{2F_{TJ}eV}{R} \coth \frac{F_{TJ}eV}{2k_B T}, \quad (1)$$

for TJs, and

$$S_I(V) = \frac{2F_{MJ}eV}{R} \coth \frac{3F_{MJ}eV}{2k_B T} + \frac{8}{3} \frac{k_B T}{R} \quad (2)$$

for MJs, where k_B is the Boltzmann constant and $F_{TJ,MJ}$ are the Fano factors. These equations generalize the dependences expected for FLs [26, 36], described by $F_{TJ} = 1$, $F_{MJ} = 1/3$, to arbitrary Fano factors.

All the studied junctions exhibit anomalously large Fano factors close to even multiples (2, 4, 6, and 8) of values expected for the FLs (Fig. 3(a)-(d) and SM). Furthermore, the Fano factors in TJs are doubled at small V , which is reminiscent of the increase from $F = 1$ to $F = 2$

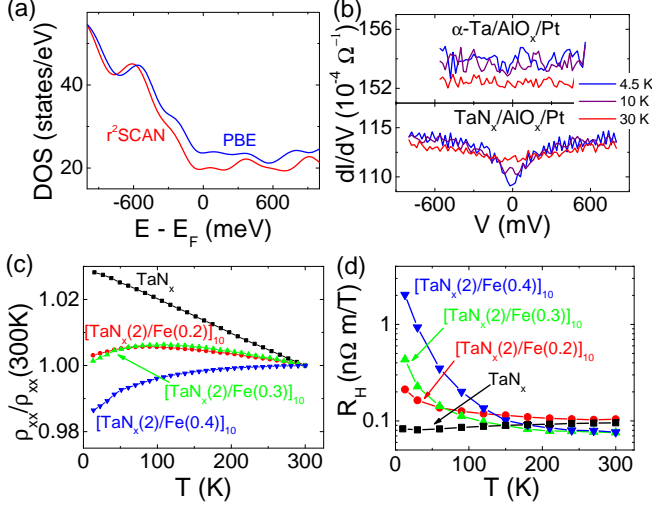


Figure 4. (a) DOS of β -Ta calculated using the r^2 SCAN mGGA and PBE functionals. (b) Conductance spectra of TaN_x and α -Ta PCs. (c) Resistivity and (d) Hall coefficient of Ta/Fe multilayers vs T .

in SC TJs at bias below the SC gap [27, 31]. These features show an overall symmetry with respect to the bias polarity.

To confirm the importance of even values of F , we define the Fano factor for individual data points as $F_{TJ} = S_I R / 2eV$ for TJs, and $F_{MJ} = (S_I R - 8k_B T / 3) / 2eV$ for MJs. The offset in the latter expression accounts for thermal contribution which is larger in MJs due to smaller F . The calculated distribution of F is quasi-continuous due to spectroscopic features and thermal broadening at small V , Figs. 3(e),(f). Nevertheless, both F_{TJ} and $3F_{MJ}$ cluster around even values.

Because of the lattice complexity and multi-orbital electronic structure, it is impractical to perform precise many-body simulations that could verify whether anomalous SN in β -Ta may be caused by correlations. We performed first principles band structure calculations based on the Perdew-Burke-Ernzerhof (PBE) and r^2 strongly constrained and appropriately normed (r^2 SCAN) meta-generalized gradient approximation (mGGA) functionals. Neither approximation captures many-particle effects [39], but the latter better accounts for correlations [40, 41]. Thus, their differences can provide insight into correlations. The density of states (DOS) calculated using r^2 SCAN is reduced near the Fermi energy compared to the PBE functional, Fig. 4(a). Comparing the calculated band structures (see SM), this is associated with the overall shift of the bands away from the Fermi surface, consistent with the effects of correlations.

DOS suppression in β -Ta was confirmed by point-contact (PC) spectroscopy. The PCs were fabricated from multilayers similar to those in SN measurements, except the MgO barrier was replaced by sputtered AlO_x

($t_B = 3.5 \text{ nm}$) and annealing was not performed, resulting in metallic point-contacts (PCs) through pinholes in AlO_x . Additionally, the TaN_x layer on top of AlO_x was replaced by Pt, so that the PC spectra were determined entirely by the electronic structure of the bottom electrode, either TaN_x or α -Ta. The latter was grown by sputtering without N_2 [42].

The differential conductance of a PC based on α -Ta is independent of bias, as expected for weakly energy-dependent DOS in the FL, Fig. 4(b). In contrast, the conductance of PC based on β -Ta decreases at small bias, which becomes more pronounced at lower T . The variation occurs on a significantly larger bias scale than in MgO (Fig. 2(b)) and Al/ AlO_x /Al TJs (see SM), and conductance is significantly higher than in TJs. This cannot be explained by tunneling effects but is consistent with reduced DOS near the Fermi level. The symmetric PC spectra do not reflect the asymmetry of the calculated band structure [Fig. 4(a)], confirming that the single-electron band approximation is inadequate.

Anomalous properties of bad metals have been attributed to the correlated Bose liquid of incoherent Cooper pairs [11]. We tested this hypothesis by introducing a proximity-induced effective exchange field via magnetic impurities, in multilayers with the structure $[\text{TaN}_x(2)\text{Fe}(t_{Fe})]_{10}\text{AlO}_x(3)$ where t_{Fe} ranged between 0.2 nm and 0.4 nm. The films were annealed in vacuum at 300° for 2 hours to promote the formation of magnetic nanoclusters. In contrast to TaN_x , these films exhibit a positive TCR at cryogenic T , with the crossover temperature to negative TCR that increases with t_{Fe} , Fig. 4(c). This cannot be explained by the parallel conductance through Fe, in which case the opposite temperature dependence would be observed due to saturation of Fe resistivity at cryogenic T . The onset of positive TCR coincides with the enhancement of Hall coefficient (Fig. 4(d)), as expected from the anomalous Hall contribution due to the onset of magnetism in Fe clusters. We conclude that “bad” metallicity is suppressed by magnetism, supporting its origin from Cooper pair-like correlations. The large magnitude of effective exchange field $\sim 10^4$ Tesla needed to suppress this state indicates that the correlations are short-ranged.

Discussion. Our central result is the observation of enhanced SN in TaN_x nanojunctions, suggesting a correlated state. First, we discuss potential alternatives. Enhanced noise cannot be an artifact due to flicker noise (FN), as we do not observe any correlation between F and FN among different samples, and the largest enhancement of F in TJs is at small bias where FN is negligible. Cooper pair tunneling in SC junctions results in doubled F , and Andreev reflections due to SC gap can further enhance SN [43]. However, this mechanism is not relevant to gapless non-SC β -Ta.

SN enhancement in TJs can be caused by intermittent blocking of tunneling through a localized state in the bar-

rier, due to interaction with another localized state [44–46]. However, analysis shows that this mechanism generally results in asymmetric dependence on bias direction, and even exceptional cases where it is symmetric F should continuously evolve with bias, inconsistent with our results (see SM for details).

We now propose a microscopic model for our observations. Each atom in β -Ta is coordinated by 20 nearest or next-nearest neighbors within a narrow distance range $d = 0.28 - 0.284$ nm [47], resulting in a low-symmetry but almost isotropic crystal field. Large spin-orbit coupling (SOC) splits the $5d$ levels into the $J = 5/2$ sextuplet and $J = 3/2$ quadruplet. The latter is occupied by the three valence electrons, consistent with the measured charge density of 1 hole per atom.

To analyze the electronic properties of β -Ta, we calculate the Koster-Slater amplitudes for hopping among the $J = 3/2$ states. These amplitudes are determined by two matrix elements, $V_1 = V_{dd\sigma} + V_{dd\pi} - 2V_{dd\delta}$, $V_2 = 2(V_{dd\pi} + 4V_{dd\delta})$, where $V_{dd\sigma} = 6V_{dd\delta} = -3V_{dd\pi}/2$ in the atomic sphere approximation [48, 49] (see SM). Both V_1 and V_2 vanish, so only hybridization beyond this approximation contributes to hopping. Hopping suppression is evident from the small bandwidths $2t \lesssim 0.5$ eV in the first-principles calculations (see SM), significantly smaller than the Mott-Hund’s energy $U = 2 - 3$ eV [50].

Strong interactions in multi-orbital systems are known to result in correlated states [51], but pairing is unexplored. Generally, the condition $t \ll U$ implies that charge fluctuations are suppressed by interaction, i.e. charges are quasi-localized even though MIT is prevented by the multi-orbital effects. The kinetic energy of holes quasi-localized on the neighboring sites is reduced by maximizing virtual hopping, which for a single orbital results in the singlet valence bond (VB) correlations that can be interpreted as quasi-localized Cooper pairs. This scenario is not directly applicable to the $J = 3/2$ quadruplet. However, the low-symmetry crystal field splits the quadruplet into two Kramers pairs and reduces SOC spin-mixing due to the hybridization with the $J = 5/2$ states. Consequently, single orbital-like pseudo-spin SOC VB correlations are expected, explaining the observed competition with ferromagnetism. A similar mechanism was proposed for SrIrO_3 , which also exhibits negative TCR at cryogenic T [36].

We argue that VB-like correlations favor bunched tunneling of even-numbered groups of holes, via the mechanism analogous to charge blockade by localized states in the tunnel barrier but involving quasi-localized holes at the interface. In contrast to Bloch states, tunneling of quasi-localized particles is likely dominated by atomic-scale hot-spots. If a hole tunnels out of such a hot-spot, the neighboring hole paired to this site by a VB (and which has a large amplitude on this site) is in a higher-energy state due to the lost correlation energy, resulting in an increased probability of its tunneling, as illustrated

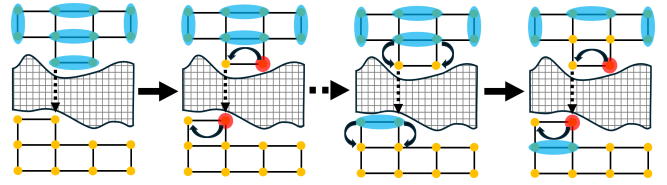


Figure 5. Correlated tunneling of holes through a hot-spot. The blue ovals are VB-like paired states, the red circles are unpaired holes. The dashed arrows indicate tunneling, curved arrows indicate hopping in the electrodes.

in Fig. 5. As both holes tunnel, other holes are attracted into the hot-spot by Coulomb effects leading to a cascade of pair tunneling.

The characteristic number of bunched electron pairs is likely determined by the local environment in the disordered metal, resulting in different values of F among the junctions. Furthermore, dynamical disorder should result in reduced bunching, consistent with decreasing F when T is increased (Fig. 2). Local measurements such as scanning SN microscopy [28] can further elucidate this mechanism.

Summary. We presented evidence for a correlated state of quasi-localized electrons manifested by anomalous SN in junctions of a disordered “bad” metal β -Ta. “Bad” metals include a variety of functional materials, among them superconductors with low kinetic inductance and relatively high T_c desirable for photon detectors and quantum information science applications [52–55]. Importantly, the symmetry of VB-like singlets due to Mott-Hund’s interactions identified in our analysis is the same as that of phonon-mediated Cooper pairs. Thus, superconductivity can be enhanced in these materials by unconventional contributions [56].

Our results have significant implications for spin-orbitronics. The single-particle band picture of SHE is not applicable to the correlated quasi-localized holes in β -Ta. Remarkably, α -Ta, which is a normal FL, exhibits almost negligible SHE. The relation between “bad” metallicity and spin-orbitronic efficiency is supported by the order of magnitude enhancement of SHE in Pt alloys approaching the Ioffe-Regel limit [57, 58]. Our analysis indicates that small crystal field effects experienced by quasi-localized electrons enable unquenched atomic orbital moments and consequently a large orbital Hall effect, and thus SHE. The effects of electron correlations on SHE can facilitate efficient correlated orbitronic and spin-orbitronic materials, warranting further studies.

Acknowledgments. We thank Connie Roth and James Merrill for assistance with spectroscopic ellipsometry. Experiments (Y.Z. and S.U.) were supported in part by the SEED award from the Research Corporation for Science Advancement. Simulations (C.X. and Y.W.) were supported by the U.S. DOE Office of Science BES

Early Career Award No. DE-SC0024524. The simulations used resources of the National Energy Research Scientific Computing Center, a U.S. DOE Office of Science User Facility at Lawrence Berkeley National Laboratory operated under Contract No. DE-AC02-05CH11231.

* yiou.zhang@emory.edu

† Also at Department of Physics and Astronomy, Clemson University, SC 29631, USA

- [1] J. G. Bednorz and K. A. Müller, *Rev. Mod. Phys.* **60**, 585 (1988).
- [2] S. Ono, Y. Ando, T. Murayama, F. F. Balakirev, J. B. Betts, and G. S. Boebinger, *Phys. Rev. Lett.* **85**, 638 (2000).
- [3] Y. Ando, G. S. Boebinger, A. Passner, T. Kimura, and K. Kishio, *Phys. Rev. Lett.* **75**, 4662 (1995).
- [4] S. C. Riggs, J. B. Kemper, Y. Jo, Z. Stegen, L. Balicas, G. S. Boebinger, F. F. Balakirev, A. Migliori, H. Chen, R. H. Liu, and X. H. Chen, *Phys. Rev. B* **79**, 212510 (2009).
- [5] S. Sahoo, U. Dutta, L. Harnagea, A. K. Sood, and S. Karmakar, *Phys. Rev. B* **101**, 014514 (2020).
- [6] H. Lin, J. Si, X. Zhu, K. Cai, H. Li, L. Kong, X. Yu, and H.-H. Wen, *Phys. Rev. B* **98**, 075132 (2018).
- [7] Y. Cao, D. Chowdhury, D. Rodan-Legrain, O. Rubies-Bigorda, K. Watanabe, T. Taniguchi, T. Senthil, and P. Jarillo-Herrero, *Phys. Rev. Lett.* **124**, 076801 (2020).
- [8] Q. Li, C. He, J. Si, X. Zhu, Y. Zhang, and H.-H. Wen, *Communications Materials* **1**, 16 (2020).
- [9] L. Zhang, B. Pang, Y. Chen, and Y. Chen, *Critical Reviews in Solid State and Materials Sciences* **43**, 367 (2018).
- [10] T. Zeng, A. Hegg, L. Zou, S. Jiang, and W. Ku, *arXiv preprint arXiv:2112.05747* (2021).
- [11] X. Zhang, A. Palevski, and A. Kapitulnik, *Proceedings of the National Academy of Sciences* **119**, e2202496119 (2022).
- [12] A. Hegg, J. Hou, and W. Ku, *Proceedings of the National Academy of Sciences* **118**, e2100545118 (2021).
- [13] D. Chowdhury, A. Georges, O. Parcollet, and S. Sachdev, *Reviews of Modern Physics* **94**, 035004 (2022).
- [14] H. Kim, S. Jamali, and A. Rogachev, *Phys. Rev. Lett.* **109**, 027002 (2012).
- [15] Y. Qin, C. L. Vicente, and J. Yoon, *Phys. Rev. B* **73**, 100505 (2006).
- [16] N. P. Breznay and A. Kapitulnik, *Science Advances* **3**, e1700612 (2017).
- [17] N. P. Breznay, M. Tendulkar, L. Zhang, S.-C. Lee, and A. Kapitulnik, *Phys. Rev. B* **96**, 134522 (2017).
- [18] C. Christiansen, L. M. Hernandez, and A. M. Goldman, *Phys. Rev. Lett.* **88**, 037004 (2002).
- [19] P. Phillips and D. Dalidovich, *Science* **302**, 243 (2003).
- [20] Y. Dubi, Y. Meir, and Y. Avishai, *Nature* **449**, 876 (2007).
- [21] P. W. Phillips, *Science* **366**, 1450 (2019).
- [22] C. Yang, Y. Liu, Y. Wang, L. Feng, Q. He, J. Sun, Y. Tang, C. Wu, J. Xiong, W. Zhang, *et al.*, *Science* **366**, 1505 (2019).
- [23] V. M. Galitski, G. Refael, M. P. A. Fisher, and T. Senthil, *Phys. Rev. Lett.* **95**, 077002 (2005).
- [24] P. Hauke, M. Heyl, L. Tagliacozzo, and P. Zoller, *Nature Physics* **12**, 778–782 (2016).
- [25] L. Liu, C.-F. Pai, Y. Li, H. Tseng, D. Ralph, and R. Buhrman, *Science* **336**, 555 (2012).
- [26] Y. Blanter and M. Büttiker, *Physics Reports* **336**, 1 (2000).
- [27] F. Lefloch, C. Hoffmann, M. Sanquer, and D. Quirion, *Phys. Rev. Lett.* **90**, 067002 (2003).
- [28] K. M. Bastiaans, D. Cho, D. Chatzopoulos, M. Leeuwenhoek, C. Koks, and M. P. Allan, *Phys. Rev. B* **100**, 104506 (2019).
- [29] R. de Picciotto, M. Reznikov, M. Heiblum, V. Umansky, G. Bunin, and D. Mahalu, *Physica B: Condensed Matter* **249-251**, 395 (1998).
- [30] L. Saminadayar, D. C. Glatli, Y. Jin, and B. Etienne, *Phys. Rev. Lett.* **79**, 2526 (1997).
- [31] K. M. Bastiaans, D. Chatzopoulos, J.-F. Ge, D. Cho, W. O. Tromp, J. M. van Ruitenbeek, M. H. Fischer, P. J. de Visser, D. J. Thoen, E. F. Driessen, *et al.*, *Science* **374**, 608 (2021).
- [32] P. Zhou, L. Chen, Y. Liu, I. Sochnikov, A. T. Bollinger, M.-G. Han, Y. Zhu, X. He, I. Bozovic, and D. Natelson, *Nature* **572**, 493 (2019).
- [33] A. H. Steinbach, J. M. Martinis, and M. H. Devoret, *Phys. Rev. Lett.* **76**, 3806 (1996).
- [34] L. Chen, D. T. Lowder, E. Bakali, A. M. Andrews, W. Schrenk, M. Waas, R. Svagera, G. Eguchi, L. Prochaska, Y. Wang, *et al.*, *Science* **382**, 907 (2023).
- [35] M. Szurek, H. Cheng, Z. Pang, Y. Zhang, J. Bacsá, and S. Urazhdin, *Applied Physics Letters* **126**, 082410 (2025).
- [36] Y. Zhang, S. Pandey, S. Ivanov, J. Liu, and S. Urazhdin, *Nano Letters* **24**, 15943 (2024).
- [37] L. W. Nordheim, *Proc. R. Soc. Lond. A Math. Phys. Sci.* **121**, 626 (1928).
- [38] A. Van Der Ziel, *Physica* **16**, 359 (1950).
- [39] W. Huang, D.-H. Xing, J.-B. Lu, B. Long, W. H. E. Schwarz, and J. Li, *Journal of Chemical Theory and Computation* **12**, 1525 (2016).
- [40] J. W. Furness, A. D. Kaplan, J. Ning, J. P. Perdew, and J. Sun, *The Journal of Physical Chemistry Letters* **11**, 8208–8215 (2020).
- [41] R. Kingsbury, A. S. Gupta, C. J. Bartel, J. M. Munro, S. Dwaraknath, M. Horton, and K. A. Persson, *Phys. Rev. Mater.* **6**, 013801 (2022).
- [42] N. N. Kovaleva, D. Chvostova, A. V. Bagdinov, M. G. Petrova, E. I. Demikhov, F. A. Pudonin, and A. Dejneka, *Applied Physics Letters* **106**, 051907 (2015).
- [43] E. V. Bezuglyi, E. N. Bratus', V. S. Shumeiko, and G. Wendin, *Phys. Rev. Lett.* **83**, 2050 (1999).
- [44] S. S. Safonov, A. K. Savchenko, D. A. Bagrets, O. N. Jouravlev, Y. V. Nazarov, E. H. Linfield, and D. A. Ritchie, *Phys. Rev. Lett.* **91**, 136801 (2003).
- [45] S. Garzon, Y. Chen, and R. Webb, *Physica E: Low-dimensional Systems and Nanostructures* **40**, 133 (2007).
- [46] Y. Zhang and G. Xiao, *Phys. Rev. B* **100**, 224402 (2019).
- [47] M. Magnuson, G. Greczynski, F. Eriksson, L. Hultman, and H. Höglberg, *Applied Surface Science* **470**, 607 (2019).
- [48] O. K. Andersen, W. Klose, and H. Nohl, *Phys. Rev. B* **17**, 1209 (1978).
- [49] J. Jenke, A. N. Ladines, T. Hammerschmidt, D. G. Pettifor, and R. Drautz, *Phys. Rev. Mater.* **5**, 023801 (2021).
- [50] J. Lee, K.-H. Jin, A. Catuneanu, A. Go, J. Jung, C. Won, S.-W. Cheong, J. Kim, F. Liu, H.-Y. Kee, and H. W.

- Yeom, Phys. Rev. Lett. **125**, 096403 (2020).
- [51] L. de' Medici, Phys. Rev. B **83**, 205112 (2011).
 - [52] M. S. Osofsky, R. J. Soulen, J. H. Claassen, G. Trotter, H. Kim, and J. S. Horwitz, Phys. Rev. Lett. **87**, 197004 (2001).
 - [53] K. Wakasugi, M. Tokunaga, T. Sumita, H. Kubota, M. Nagata, and Y. Honda, Physica B: Condensed Matter **239**, 29 (1997).
 - [54] S. Mandal, S. Dutta, S. Basistha, I. Roy, J. Jesudasan, V. Bagwe, L. Benfatto, A. Thamizhavel, and P. Raychaudhuri, Phys. Rev. B **102**, 060501 (2020).
 - [55] P. Chauhan, R. Budhani, and N. P. Armitage, Phys. Rev. B **105**, L060503 (2022).
 - [56] Y.-J. Zhang, Y. Zhu, Q. Li, Z.-N. Xiang, T. Huang, J. Sun, and H.-H. Wen, Journal of the American Chemical Society **146**, 21110 (2024).
 - [57] U. Shashank, T. Tomoda, A. J. Mathew, G. Vashisht, K. Imai, Y. Kusaba, C.-L. Dong, C.-L. Chen, Y. Horibe, M. Ishimaru, H. Awano, H. Asada, and Y. Fukuma, NPG Asia Materials **17** (2025).
 - [58] Q. Liu and L. Zhu, arXiv preprint arXiv:2506.06628 (2025).